Mater. Res. Soc. Symp. Proc. Vol. 1290 © 2011 Materials Research Society
DOI: 10.1557/opl.2011.178

Structural, Magnetic and Electronic Properties of Dilute MnScN(001) Grown by RF Nitrogen Plasma Molecular Beam Epitaxy

Costel Constantin,[1] Kangkang Wang,[2] Abhijit Chinchore,[2] Han-Jong Chia[3], John Markert[3], Arthur R. Smith,[2]

[1]Department of Physics and Astronomy, James Madison University Harrisonburg, VA 22801

[2]Nanoscale & Quantum Phenomena Institute, Department of Physics and Astronomy, Ohio University, Athens, OH 45701

[3]Department of Physics, University of Texas at Austin, Austin, TX 78712

ABSTRACT

The structural, magnetic, and electronic properties of dilute Mn-doped scandium nitride thin films grown by radio frequency N-plasma molecular beam epitaxy are explored. The results indicate a small magnetization extending up to as high as 350K. There is a slight dependence on the manganese concentration, with the lower Mn concentration showing a larger saturation magnetization.

INTRODUCTION

In recent years there has been much interest in obtaining III-V dilute magnetic semiconductors (DMS's) by doping semiconductors, such as gallium nitride (GaN) and gallium arsenide (GaAs), with transition metals (TM) such as manganese (Mn). For MnGaAs, the reported values for T_C were previously limited to 110K [1], and this limit remained in place for many years. More recently, post-growth annealing treatments have made it possible to surpass this barrier, however, even with this method, T_C in MnGaAs remains around 173K [2].

After the exciting prediction of Dietl *et al.* [3] in 2000 who stated that 5% Mn concentration in GaN or ZnO can raise the T_C above room temperature, many experimental studies reported growth and magnetic properties of MnGaN [4-8]. Interestingly, these studies show that ferromagnetism including the Curie point (T_C) strongly depends on the growth mode. Haider *et al.* [7] showed that N-rich and slight metal-rich growth regimes of MnGaN result in T_C above 300K. Recently, Alexandrov *et al.* [9] reported electric field-dependent magnetic properties for MnGaN, showing a 39% decrease in saturation magnetization (M_{SAT}) with applied voltage over the range 0-5 V.

Despite some successes, it is important to realize that limitations in the rapid development of DMS materials can be related to dopant incorporation issues, and this was realized from the very beginning of DMS research. For the GaAs system, there are two types of point defects that are believed to preclude achieving very high T_C values - Mn intersitials and As antisites, both of which act as double donors. There are suspicions that difficulty for the Mn to occupy the cation sites in GaAs (and in GaN) is attributed to mismatch in bonding (octhahedral vs. tetrahedral). Mn tends towards octahedral bonding in manganese nitride - Mn_xN_y alloys mostly have rocksalt-type tetragonal structure [10] (with the exception of the ζ-phase which reportedly has hexagonal structure [11,12]), whereas cations in GaAs and GaN have tetrahedral bonding.

It is therefore of great interest to investigate DMS systems in which there is the possibility of isostructural bonding between the host semiconductor cation and the TM dopant. One such semiconductor is scandium nitride (ScN), which has octahedral bonds in a rock-salt crystal structure. Al-Brithen *et al.* [13] showed that MnScN alloy thin films followed Vegard's law, with the two tetragonal lattice parameters of the Mn-rich end linearly approaching the single cubic lattice parameter at the Sc-rich end. Recent theoretical calculations by Herwadkar *et al.* [14,15] have predicted a T_C above 350K for MnScN alloys, when ScN is doped with up to 20% Mn. It is therefore of great interest to explore this materials further. In this paper, we report a study of the structural, electronic, and magnetic properties of manganese-doped scandium nitride ($Mn_xSc_{1-x}N$) films grown by radio-frequency nitrogen plasma molecular beam epitaxy (rf-MBE).

EXPERIMENT

The $Mn_xSc_{1-x}N$ films with cation flux ratio $R = J_{Mn}/(J_{Sc} + J_{Mn}) \sim 3\%$ (sample S450) and $R \sim 5\%$ (sample S452) are grown using rf-MBE using N_2 as a source gas and employing effusion cells for both Mn and Sc evaporation. During the entire growth, the N plasma source is kept constantly operating at 500 W and with a N_2 flow rate set at 1.1 sccm ($P_{chamber} = 9 \times 10^{-6}$ Torr). The substrate temperature is measured using a thermocouple located behind the substrate heater and by using an infrared pyrometer looking through a viewport directly at the front side of the sample. The $Mn_xSc_{1-x}N$ layer is grown at a specific flux ratio R with $J_{Mn} = 4.64 \times 10^{12}$ $cm^{-2}s^{-1}$ (S450) or $J_{Mn} = 7.26 \times 10^{12}$ $cm^{-2}s^{-1}$ (S452). The $J_{Sc} \sim 1.5 \times 10^{14}$ $cm^{-2}s^{-1}$ is kept constant for the entire $Mn_xSc_{1-x}N$ film growth. During the growth, the films are monitored by reflection high-energy electron diffraction (RHEED) after which the samples are measured *ex-situ* with atomic force microscopy (AFM), thin-film measurement system (Filmetrics F20), resistivity/Hall effect measurements (R-T/Hall effect), and superconducting quantum interference device (SQUID).

DISCUSSION

In the following we discuss the results of measurements on MnScN films with a focus on two films, one grown with intentional concentration of 3% Mn, the other with intentional concentration of 5% Mn. The results are presented in the order of structural, magnetic, and electronic properties.

Structural Properties

The MgO(001) substrate is first heated to 950 °C for 30 min under the presence of N plasma, after which the RHEED pattern looks streaky [figures 1(a) and 1(b)], indicating a suitably smooth substrate surface. A buffer layer of ScN is grown at a sample temperature of 800 °C and with thickness $t_{ScN} \sim 60$ nm. The RHEED patterns of the buffer layer [figures 1(c) and 1(d)] indicate a relatively smooth starting substrate, despite being very thin.

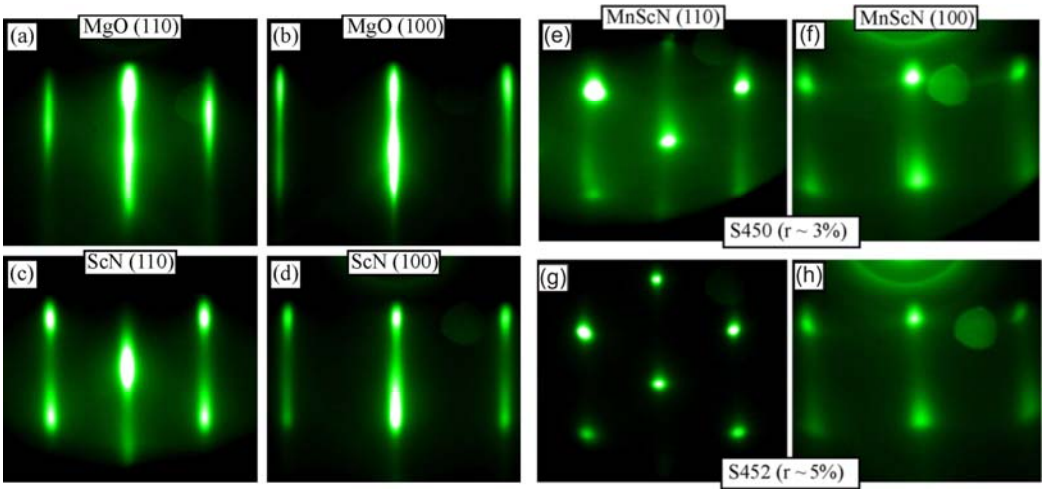

Figure 1. (a) & (b) RHEED patterns of MgO(001) substrate taken along [110] and [100] crystal orientation; (c) & (d) RHEED patterns of ScN(001) buffer layer taken along [110] and [100] crystal orientation. (e – h) RHEED patterns of samples 450 and 452, showing spot-like patterns, but with fct crystal structure, indicative of a crystalline film with a rough surface.

Next, the substrate temperature is decreased to $T_S \sim 420$ °C and the $Mn_xSc_{1-x}N$ layer is grown. RHEED patterns for samples S450 and S452 are displayed in figure 1 (e – f). These RHEED patterns are obtained ~ 1 min. before the end of the $Mn_xSc_{1-x}N$ layer growth. The thickness of the $Mn_xSc_{1-x}N$ layers were measured with thin-film measurement system Filmetrics F20 and we found for sample S450 a thickness of $t_{S450} \sim 440$ nm, and for sample S452 a thickness of $t_{S452} \sim 450$ nm, respectively. Qualitatively, both samples show a spotty RHEED pattern behavior indicating 3-dimensional growth. The symmetry of the spot pattern is face-centered tetragonal. The patterns are somewhat spottier than earlier observations at the growth temperature of 420 °C and may indicate a lower true growth temperature [13].

Atomic force microscopy images for samples S450 and S452 are presented in figure 2. It is seen that both samples have a rough surface, consistent with the spotty RHEED patterns. The RMS roughness values measured for the 5 μm × 5 μm images presented in figure 2 for samples S450 and S452 are 7.1 nm and 6.4 nm, respectively. Previous ScN(001) growth studies on MgO(001) substrates revealed atomically smooth films as investigated by scanning tunneling microscopy measurements, for both N-rich and Sc-rich cases [16,17]. The smooth topography could also be seen in AFM images. It is notable however, that the smooth growth of ScN is optimized at temperatures even higher than that for GaN, namely in the range of 800-850 °C. In order to incorporate Mn, it is necessary to reduce the growth temperature to not more than 518 °C [13]. A low growth temperature for ScN produces a rougher ScN growth morphology due to reduced surface diffusion. However, despite the roughness of the surface seen in the AFM images (figure 2), there is no obvious indication of significant amounts of precipitation of metallic constituents at the surface. It should be noted that it was previously reported that MnScN growth at higher Mn flux values (R ~ 19%) results in some precipitation at a growth temperature of 424 °C, but even in that case incorporation of Mn into Sc sites of the ScN lattice is also definitely observed [13]. For the case here of very low Mn concentration (R ~ 3-5%), the precipitation is not obvious in AFM images.

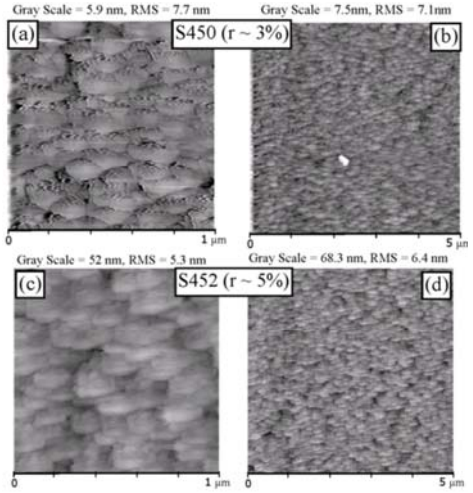

Figure 2. Atomic force microscopy images of samples S450 and S452. Image sizes are 1×1 μm^2 (a and c) and 5×5 μm^2 (b and d).

Magnetic Properties

To analyze the magnetic behaviour of these films, SQUID magnetization vs. applied field measurements were performed, as presented in figure 3. The raw data has been corrected by performing a background subtraction of the paramagnetic signals which originate from the sample holder and the substrate. Both samples S450 and S452 show hysteresis with saturation at 0.746 emu/cm^3 and 0.309 emu/cm^3, respectively. Saturation is achieved at ~ 2500 Oe for both samples. While the 3% intentional-doped sample (S450) does not show any measurable remanent magnetization, the 5% intentional-doped sample (S452) shows about 0.044 emu/cm^3 at remanence and a coercive field of about 425 Oe.
We also performed measurements on a ScN film (as a control sample) which did not have any Mn doping (S446). After subtraction of a linear paramagnetic background, the magnetization of the ScN sample is a small offset value which varies only slightly with applied field and has negligible (or no) hysteresis. Comparing to the signals shown in figure 3(a) and 3(c), it confirms that the Mn-doped samples' magnetizations are due to the presence of Mn in the films.

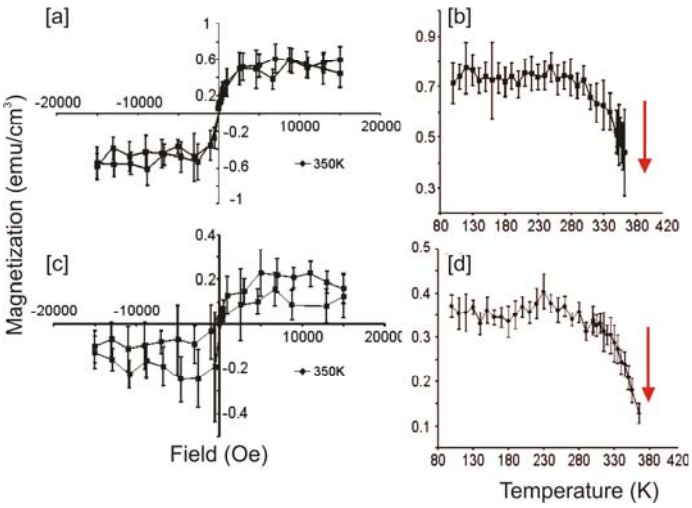

Figure 3. Magnetization versus field, and temperature for samples S450 [(a) & (b)], and S452 [(c) & (d)], respectively.

Magnetization versus temperature measurements for the two samples S450 and S452 are presented in figure 3 (b) and (d), respectively. These measurements were done under an applied field of 20,000 Oe. Both samples clearly show net magnetization from low temperatures all the way up to above room temperature, with transition points close to 365 K. We calculated the magnetic moment per atom for S450 and S452 assuming 3% and 5% incorporation respectively, obtaining $\mu^{(S450)} = 0.0617\ \mu_B$/ Mn-atom, and $\mu^{(S452)} = 0.0152\ \mu_B$/ Mn-atom ($\mu_B = 9.724 \times 10^{-21}$ emu). Although being small moments, interpretation of the magnetization as being due to a dilute incorporation of Mn atoms leading to cooperative spin polarization within the ScN semiconductor material is a possibility. It is also possible that the actual incorporation is less than the flux ratio *R*, as observed and reported by Al-Brithen [13]; if so, these magnetic moment per atom values would be underestimates.

To test if the magnetism could be due to MnSc metal alloy precipitation, we purposely grew MnSc alloy samples on MgO(001). But we find that Mn_xSc_{1-x} MBE grown films with x = 3 – 15% show no ferromagnetism. Other possible sources of magnetization could include Mn-Mn clustering, ferrimagnetic ε-phase (Mn_4N) or possibly magnetic ζ-phase (Mn_2N) precipitates. Note that stoichiometric (1:1) θ-MnN is antiferromagnetic with high Neel Temperature of ~ 650 K [18, 19, 20], and as well Mn_3N_2 is antiferromagnetic with also a high Neel temperature [21]. The ζ-phase (Mn_2N) is less well-studied but reportedly also antiferromagnetic [11]. While the ε-phase Mn_4N cannot be 100% excluded, it is unlikely to be the origin of the observed magnetism given the N-rich growth conditions, and since Al-Brithen *et al.* [13] clearly demonstrated Vegard's law behavior for MnScN up to r ~ 26 % Mn, proving the solubility and incorporation of Mn into ScN at suitable temperatures. The measured magnetic moment per Mn atom appears to be significantly smaller, however, than that predicted theoretically. Both Herwadkar *et al.* [15] and Houari *et al.* [22] reported magnetic moments per Mn atom of ~ 3 μ_B/Mn-atom and higher. Despite these differences, the experimental results suggest the existence of a spin polarization which extends to above room-temperature for dilute MnScN.

Electric Properties

Preliminary measurements using Hall Effect and resistivity vs. temperature were performed using a home-made four-point probe Van der Pauw system. The carrier concentration was determined to be $n_S^{(S450)} = 4 \times 10^{19}$ /cm^3, and $n_S^{(S452)} = 2.18 \times 10^{19}$ /cm^3, with corresponding mobility $\mu_S^{(S450)} = 24.8$ cm/(Vs), and $\mu_S^{(S452)} = 33.8$ cm/(Vs). For a ScN control sample, $n_S = 2.76 \times 10^{20}$/cm^3, approximately 7× larger than for S450 (R = 3% intentional Mn) and more than 12× larger than for S452 (R = 5% intentional Mn). The high electron concentration for the ScN can be ascribed for the most part to N vacancies [17]. Based on these results, we find that the presence of Mn atoms has an electron-compensating effect in ScN. The drop in electron concentration can then be due to either compensation by acceptor-behaving Mn atoms or to significant reduction of N vacancies with presence of Mn; however, N vacancies are common in MnN as well as ScN, and so it is not obvious why a strong reduction of N vacancies would occur due to the presence of Mn.

CONCLUSIONS

In conclusion, we have explored the properties of dilute Mn-doped ScN grown by rf N-plasma MBE at 420 ºC and have found small but finite magnetization extending up to ~ 365 K. The RHEED and AFM measurements indicate a crystalline and relatively homogeneous-looking surface, consistent with Mn incorporation into the ScN lattice. Carrier concentration measurements suggest acceptor-like behavior for the Mn dopant atoms, which effectively compensates the normally n-type conductivity of the ScN semiconductor; this further corroborates Mn incorporation. The observed magnetization behavior suggests the possibility of cooperative magnetic interactions between dispersed Mn ions. Further study will be needed to resolve the apparent discrepancy between predicted and observed magnetic moments.

ACKNOWLEDGEMENTS

This study is supported by the Department of Energy, Office of Basic Energy Sciences (Grant No. DE-FG02-06ER46317). Additional support from the National Science Foundation (Grant Nos. 0730257 and DGE-0549417) is also acknowledged.

REFERENCES

[1] H. Ohno, Science vol. 281, 951-956 (1998).
[2] K.Y. Wang *et al.*, AIP Conf. Proc. Vol. 772, 333-334 (2005).
[3] T. Dietl, H. Ohno, F. Matsukura, J. Cibert and D. Ferrand, Science vol. 287, 1019 (2000).
[4] S. Sonoda, S. Shimizu, T. Sasaki, Y. Yamamoto, H. Hori, J. Crys. Growth vol. 237, 1358 (2002).
[5] G. T. Thaler *et al.*, Appl. Phys. Lett. vol. 80, 3964 (2002).
[6] M. E. Overberg, C. R. Abernathy, S. J. Pearton, N. A. Theodoropoulou, K. T. McCarthy, and A. F. Hebard, Appl. Phys. Lett. vol 79, 1312 (2001).
[7] M. B. Haider, C. Constantin, H. Al-Brithen, G. Caruntu, C. J. O'Conner, A. R. Smith, Phys. Stat. Solidi A 202:6, 1135 (2005).
[8] K. Sato, W. Schweika, P. H. Dederichs, H. Katayama-Yoshida, Phys. Rev. B vol 70, 201202 (2004).
[9] D. Alexandrov, Cent. Europ. J. Chemistry **7(2)**, 175 (2009).
[10] H. Yang, H. Al-Brithen, A. R. Smith, E. Trifan, and D. C. Ingram, J. Appl. Phys. **91(3)**, 1053 (2002).
[11] M. Mekata, J. Phys. Soc. of Japan **25**, 234 (1968).
[12] A. Leineweber, J. Alloys & Compounds **368**, 229 DOI 10.1016/j.jallcom.2003.08.062 (2004).
[13] H. A. AL-Brithen, H. Yang, A. R. Smith, J. Appl. Phys. 96(7), 3787 (2004).
[14] A. Herwadkar, W. R. L. Lambrecht, Phys. Rev. B 72 (23), 235207 (2005).
[15] A. Herwadkar, W. R. L. Lambrecht, M. van Schilfgaarde, *Phys. Rev. B 77, 134433 (2008).*
[16] H. Al-Brithen, A. R. Smith, Appl. Phys. Lett. **77**, 2485 (2000).
[17] A. R. Smith, H. A.H. AL-Brithen, D. C. Ingram, D. Gall, J. Appl. Phys. **90(4)**, 1809 (2001).
[18] R. Yang, M. B. Haider, H. Yang, H. Al-Brithen, A. R. Smith, A-Mat. Sci. & Process. 81(4), 695 (2005).
[19] A. Leineweber, R. Niewa, H. Jacobs, and W. Kokelman, J. Materials Chemistry 10:(12), 2827 (2000).
[20] K. Suzuki, T. Kaneko, H. Yoshida, Y. Obi, H. Fujimori, H. Morita, J. Alloys and Compounds 306, 66 (2000).
[21] H. Yang, H. Al-Brithen, A. R. Smith, J. A. Borchers, R. L. Cappelletti, M. D. Vaudin, Appl. Phys. Lett. 78, 3860 (2001).
[22] A. Houari, S.F. Matar, M. A. Belkhir, Comp. Mat. Sci. 43 (2), 392 (2008).